DOI: 10.1002/stco.202300025

Sheida Afshan, Weiran Li, Zhenzhou Wang, Wendell Bailey, Yikun Wang

REPORT

High-performance metallic materials for applications in infrastructure and energy sectors

Keynote at Eurosteel 2023 in Amsterdam

High performance steels, such as stainless steels, have many desirable characteristics that warrant their use in various sectors, including infrastructure and energy applications. This paper is concerned with two of such applications: (i) the use of stainless steel for large-scale liquid hydrogen storage tanks, which is a requirement for the future hydrogen energy network, and (ii) the use of stainless steel in steel-framed buildings to enhance their robustness under extreme loading conditions. The paper begins with a discussion of the technical challenges associated with the material behaviour of stainless steel storage tanks under extreme temperature and pressure conditions. It presents and discusses the results of a pilot experimental programme that investigates the mechanical behaviour of stainless steel 304 L material under cryogenic 20 k hydrogen environment. Next, to demonstrate the benefits of the strategic use of stainless steel in the key connection parts of steel-framed structures, the paper presents the setup for a new test programme that investigates the behaviour of stainless steel beam-to-column connections, using A4-70 bolts and EN1.4301 plates, under a column removal scenario. The numerical modelling prediction results of the specimens are presented, and comparisons with carbon steel counterparts are made and discussed.

Keywords hydrogen storage; infrastructure; resilience; robustness; stainless steel; sustainability

1 Introduction

High performance metallic materials offer many opportunities for applications in the infrastructure and energy sectors, accelerating the progress towards global sustainability, resilience and achieving net-zero targets. Stainless steels has many desirable characteristics, including enhanced mechanical properties such as high strength and ductility as well as high corrosion resistance, making it the material of choice for applications that demand durability and high performance. This paper presents the current research works related to such two applications: (i) the use of stainless steel for large-scale liquid hydrogen storage tanks, which is a requirement for the future hydrogen energy network, and (ii) the use of stainless steel in steel-framed buildings to enhance their robustness under extreme loading conditions.

2 Stainless steel for liquid hydrogen storage tanks

Decarbonisation is the most urgent task faced globally to mitigate the climate emergency and sustain standards of living. As part of a decarbonised and renewable energy system, low-carbon hydrogen provides a versatile replacement for high-carbon fuels used today in the energy and transportation sectors. Hydrogen is considered to play an important complementary and enabling role alongside clean electricity in decarbonising our energy systems, especially in sectors where electrification is unfeasible or too costly, and other decarbonization options are limited, such as in long-distance and heavy-duty transportation like maritime. A major advantage of hydrogen is that it can be produced from surplus renewable energy. Unlike electricity, it can be stored on a large scale for long durations, making it a viable option for energy transmission as well. The International Maritime Organization (IMO) has set a target to reduce greenhouse gas emissions from shipping by at least 50 % by 2050. Research from the Lloyd's Register Decarbonisation Hub has shown that Zero Emission Vessels (ZEVs), adopting zero carbon energy sources and technologies such as hydrogen, are necessary to meet the IMO's target. The UK government (Hydrogen Strategy-2021) [1] and industry have identified hydrogen as one of the major fuels for zero emission transportation and energy supply; it envisages offshore production of green hydrogen (from wind) for maritime transport to shore terminals, similar to today's LNG system. However, one of the main obstacles in the uptake of hydrogen fuel is the lack of policies and regulations related to the technical design and approval of hydrogen fuel technology systems in different transport operating environments. One imminent area is storage technologies for hydrogen as an energy carrier, especially in maritime transportation. To address this, research is currently underway at the University of Southampton to investigate the use of stainless steel metallic cylinders for hydrogen storage in large-scale maritime applications. Stainless steel, particularly the austenitic grade, has desirable characteristics for low-temperature and high-pressure hydrogen storage. This section presents the results of a pilot programme of novel experimental testing that investigates the material performance of stainless steel under cryogenic hydrogen environment.

2.1 Hydrogen storage methods

Hydrogen is stored under high-pressure and low-temperature conditions to increase its energy density. Figure 1 com-

 ,

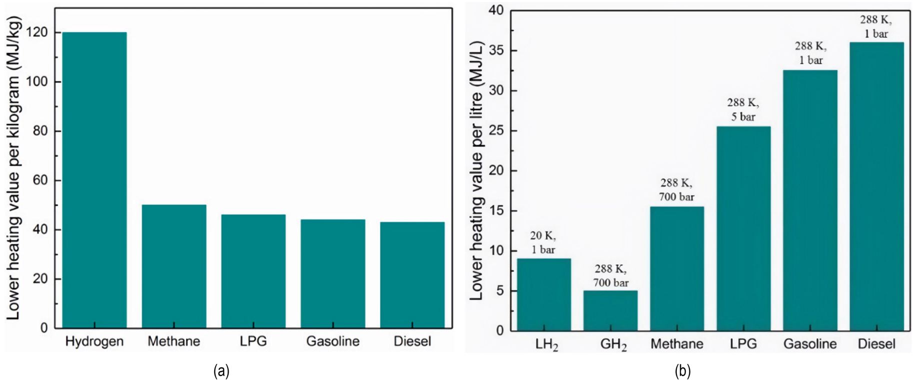

Fig. 1 Comparison of the energy density of hydrogen with hydrocarbon fuels [2]; a) gravimetric energy density, b) volumetric energy density

pares the gravimetric and volumetric energy densities of hydrogen with other fuels. While the gravimetric energy density, i.e., the energy per unit mass, of hydrogen is more than double that of methane, liquid petroleum gas (LPG), gasoline and diesel hydrocarbon fuels, its volumetric energy density, i.e., energy per unit volume, in both liquid and compressed forms, is the lowest. This means that storing hydrogen fuel would require comparatively larger tank sizes and they would need to be designed to withstand the extreme low-temperature and high-pressure environments necessary for liquid and gaseous hydrogen storage. Amongst the different hydrogen storage methods, physical-based storage methods provide the most viable option for large-scale storage applications, such as in maritime transportation. Physical-based methods mainly consist of three storage types: liquid hydrogen (LH2), cryo-compressed hydrogen (CcH2) and compressed gaseous hydrogen (GH2). Figure 2 compares the temperature, pressure and energy densities of LH2, CcH2 and GH2. The storage conditions for liquid hydrogen, which is the focus of the current paper, range from 20 to 33 Kelvin (K) in temperature and 1 to 12.76 bar in pressure, offering the highest volumetric energy density compared to the CcH2 and GH2 forms.

2.2 Metallic materials for LH2 storage

Specialist tanks or storage vessels, purpose built using materials capable of safely containing hydrogen at the required temperatures and pressures, are considered as a viable option for large-scale hydrogen fuel storage and transportation. Storage vessels offer lower upfront costs compared to other methods and can be installed or deployed more quickly [3]. Currently, there are over 10 vessels with hydrogen fuel cells on board, but most of them are small river boats and ferries at the concept-proving stage [2]. Scaling up this technology for ocean-going ships and hydrogen carriers faces challenges due to the lack of a unified agreement or understanding regarding the behavior of materials used for hydrogen containment in service environments on ships. The absence of codes and standards reflects the industry's lack of confidence in hydrogen storage and usage on board ships. The choice of material for hydrogen storage tanks, especially in the liquefied state at 20 K (−253 °C), involves various considerations such as low-temperature embrittlement, hydrogen embrittlement, failure mode, thermal contraction and the effects of metallurgical instability. High-alloy austenitic stainless steel is commonly used in hydrogen environments and has been used for constructing liquid hydrogen tanks since 1950s by NASA. However, there has been limited experimental testing focused on determining the suitability of austenitic stainless steels, including grades 304 L and 316 L, for carrying and storing liquid and compressed hydrogen on board ships. To address this knowledge gap, a research project is currently underway at University of Southampton to comprehensively characterise the material behaviour of different types of austenitic stainless steels, including grades 304 L and 316 L, in cryogenic hydrogen environments. The change in the key mechanical properties, such as the tensile stress-strain response and fracture toughness behaviour, of the base material as well as the weld and the heat affected zone (HAZ) when exposed to cryogenic hydrogen-containing environment will be investigated.

2.3 Pilot experimental investigation

2.3.1 Experimental setup

An experimental programme was conducted to measure the tensile stress-strain behaviour of stainless steel 304 L materials under cryogenic temperature and hydrogen environment.

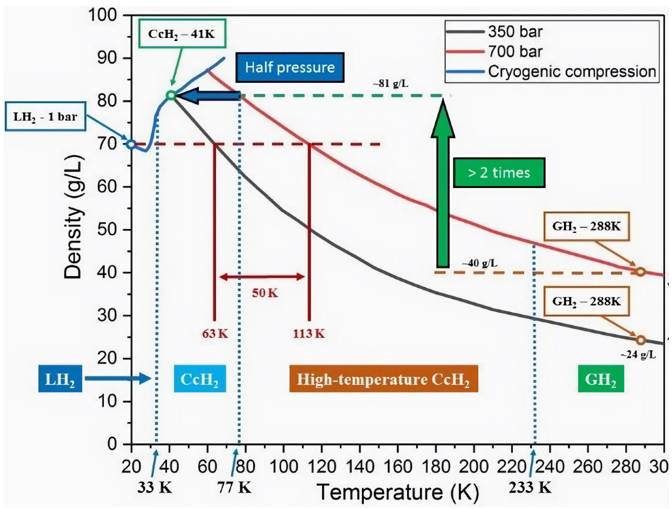

Fig. 2 LH2, CcH2 and GH2 energy density comparisons [2]

The specimens were machined into dog-bone shape coupons and were tested in three different conditions, which were (i) at room temperature (RT) without prior hydrogen conditioning, (ii) at cryogenic temperature 20 K (CT) without prior hydrogen conditioning and (iii) at cryogenic temperature 20 K with prior hydrogen conditioning. The hydrogen conditioning was conducted at 2 bars hydrogen gas pressure since it was considered as a conservative representation of the environment within liquid hydrogen containment. The mechanical tests were conducted in the Testing and Structure Research Laboratory (TSRL) at University of Southampton in accordance with the ISO 6892-4 [4] cryogenic testing standard. The tensile tests were performed in a purpose-built test rig which was fitted within a 50 kN Instron 3369 servo-mechanical universal testing machine as shown in Fig. 3a. A bespoke conditioning chamber made of a silvered vacuum insulated glass Dewar was used to create the required 20 K test temperature as shown in Fig. 3b. Cryogenic nitrogen gas and cryogenic helium gas were injected into the conditioning chamber to cool down the test specimens to a target temperature of 20 K using the arrangement shown in Fig. 3c. The cooling process was executed in two steps. In the first step, boiled cryogenic nitrogen gas was injected into the glass Dewar to reduce the sample temperature from room temperature to 80 K. In the second step, cryogenic helium gas was flown into the glass Dewar to further reduce the temperature from 80 K to 20 K. The temperature in the locality of the coupon specimens was measured and recorded prior to the start of the tensile test with a calibrated Epsilon cryogenic rhodium-iron thermometer. A calibrated 50 kN load cell was used to measure the applied load. The tests were conducted in displacement control with the crosshead displacement rate of 1 mm/min.

2.3.2 Experimental results and discussions

The measured engineering stress-strain curves at room temperature (RT) and cryogenic temperature (CT) 20 K are shown in Fig. 4a,b, respectively. The key mechanical properties of each coupon are summarised in Tab. 1, where E is the Young's modulus, $f_{0.2}$ is the 0.2 % proof stress, f_u is the ultimate tensile strength, ε_u is the strain at ultimate tensile strength and ε_f is the strain at fracture. The room temperature stress-strain curves display a rounded response with no clearly defined yield point and strain-hardening as expected for the grade 304 L material [5]. There is also a good agreement between the repeated tests as shown in Fig. 4a. The stress-strain characteristics at cryogenic temperature are however completely different to those at room temperature. As shown in Fig. 4b, the shape of the stress-strain relationship changes to a linear response up to an upper yield point, followed by a yield plateau before the onset of strain-hardening and final fracture. The stress-strain responses of the hydrogen conditioned and unconditioned specimens show similar responses, which is considered to be due to the negligible concentration of absorbed hydrogen under the adopted hydrogen charging conditions. The 20 K responses exhibit a substantial increase in the yield strength and the ultimate tensile strength and a reduction in the ductility, in terms of both the ultimate strain and the fracture strain, compared to the room temperature response. The ultimate tensile strengths of all the tested coupons at 20 K increased by over two times compared with the room temperature values – the mean ultimate tensile strength was 695 MPa at room temperature and 1594 MPa at 20 K. The mean yield strength increased by a lower amount from 463 MPa at room temperature to 583 MPa at 20 K. In addition, as illustrated in

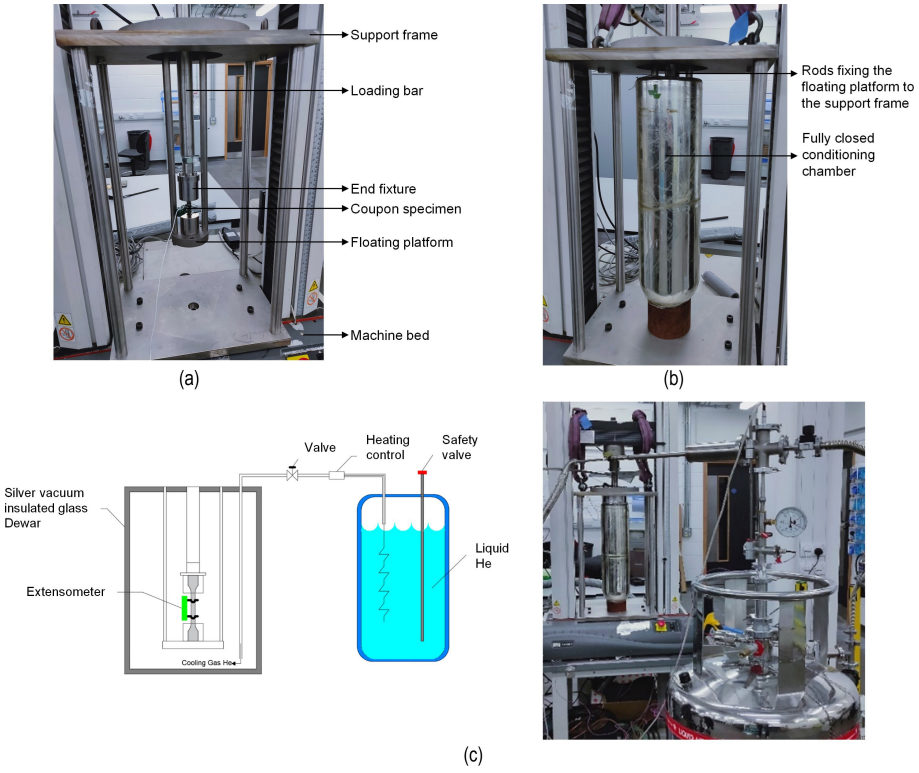

Fig. 3 Arrangement of the tensile test setup and the adopted nitrogen and helium gas cooling system; a) specimen and test rig arrangement; b) fully closed conditioning chamber; c) nitrogen and helium gas cooling system

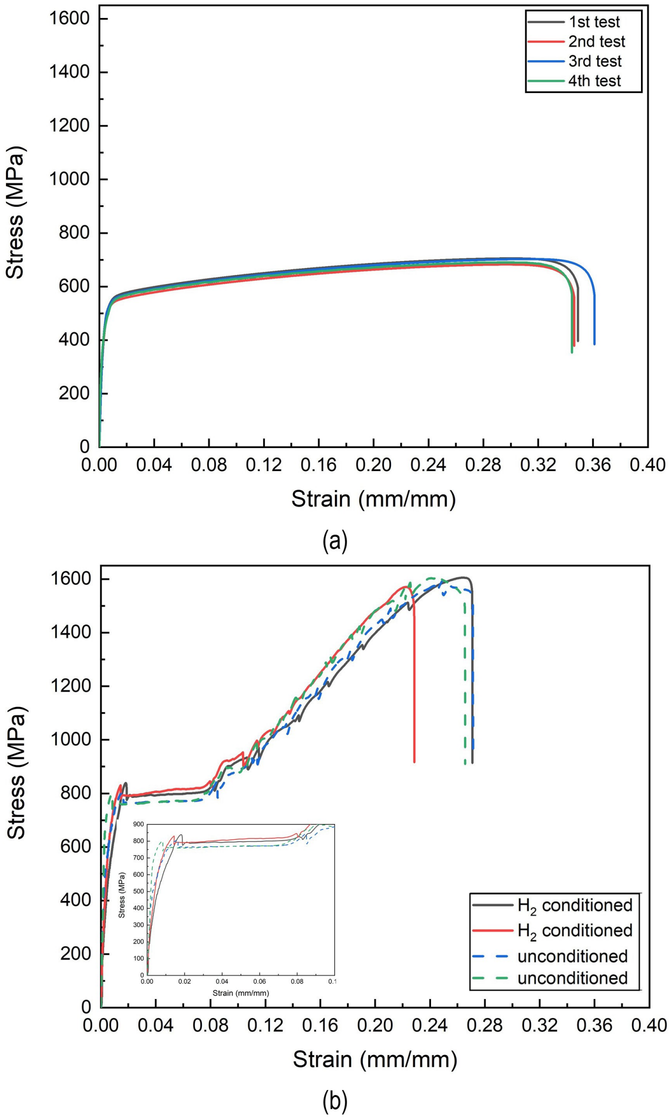

Fig. 4 The measured stress-strain curves at (a) room temperature and (b) 20 K

Fig. 4b, the fracture strains of all the coupons at 20 K were lower, on average by 27 %, than those at room temperature. The mean fracture strain was 0.35 at room temperature and 0.25 at 20 K.

The above-described changes in the shape of the measured stress-strain curve and the increase in the tensile strength at cryogenic temperatures are attributed to the combined effects of low temperature and plastic strain-induced martensitic transformation [6–9]. At low temperature, the dislocations motion becomes difficult in austenitic stainless steels. In addition, during the phase transformation, the γ-austenite phase changes to α′-martensite phase, which acts as a reinforcing phase by constraining the slipping of the dislocations causing the increase in the strength. The critical plastic strain at which the martensite transformation initiates has been shown to reduce with decreasing temperatures [7], meaning that the above-described changes in the material behaviour become more prominent at lower temperatures. This is because the stacking fault energy of the austenite phase reduces with decreasing temperature, it becomes unstable and smaller plastic deformation and/or mechanical force is required to initiate the martensite transformation [7,8]. Accurate predictions of the above-described changes in the material behaviour and ability to model the stress-strain response are important for the design and safety assessment of liquid hydrogen storage tanks. Further tests on different stainless steel grades of base, weld and heat affected zones are currently underway to further investigate the effects of cryogenic temperature and hydrogen permeation on the mechanical behaviour of the material.

3 Stainless steel for enhanced robustness of structural frame systems

There is a critical need for new and existing infrastructure to be resilient to the more frequent extreme conditions that they now face – fires, explosions, aging infrastructure, etc. – as well as the parallel challenges associated with climate change e. g. more extreme and unpredictable loading on structures. Key to the resilience of steel-framed buildings under any form of extreme load is a robust and ductile structural frame, especially at the joints. Structural joints are required to undergo considerable inelastic rotations and accommodate high tying forces at large deflections during an extreme event, thus allowing beams to develop catenary action and provide alternative load paths in the case of a sudden column loss. In that respect, the use of a high performance metallic material, such as stainless steel which has greater ductility and energy absorption, in the joint locations can play a key role in enhancing the robustness of new and rehabilitated steel frame structures. An experimental testing programme investigating the behaviour of stainless steel bolted connections under a column removal scenario is cur-

Tab. 1 Summary of measured key mechanical properties

Temperature	E (MPa)	$f_{0.2}$ (MPa)	f_u (MPa)	ε_u (mm/mm)	ε_f (mm/mm)
Room temperature without H2	200000	469	705	0.296	0.347
	196000	456	683	0.292	0.344
	179000	483	703	0.307	0.359
	208000	445	690	0.291	0.343
Cryogenic temperature with H2	178000	444	1606	0.256	0.266
	183000	580	1571	0.214	0.224
Cryogenic temperature without H2	241000	556	1593	0.242	0.268
	236000	751	1605	0.240	0.262

rently underway at the University of Southampton within the framework of a collaborative research project *RESIST: resilient buildings using stainless steel.* This section presents an overview of the planned experimental investigation and the results of the pre-test predictions.

3.1 Experimental investigation

An experimental test programme has been designed to investigate and quantify the potential advantages in terms of overstrength, energy absorption and ductility that result from the adoption of highly ductile stainless steel components in critical parts of the steel joints, such as the end plates, angle cleats and bolts. Fig. 5 shows the configuration of the frame sub-assembly column removal tests. The two-sided joints comprise of stainless steel connections and carbon steel beam and column members. The ends of the beams are connected to the lateral reaction frames simulating the structural continuity and provide axial restraint to the beams. For the quasi-static column removal tests, the specimens are loaded at the middle column through an actuator mounted onto the vertical reaction frame, while for the dynamic column removal tests, the middle column support system is removed suddenly. To compare the relative performance of different beam-to-column connection types, three connection configurations including double angle web cleat, top and seat angle cleat and extended end plate, representing nominally pinned, semi-rigid and rigid joints, respectively, as shown in Fig. 6, will be tested.

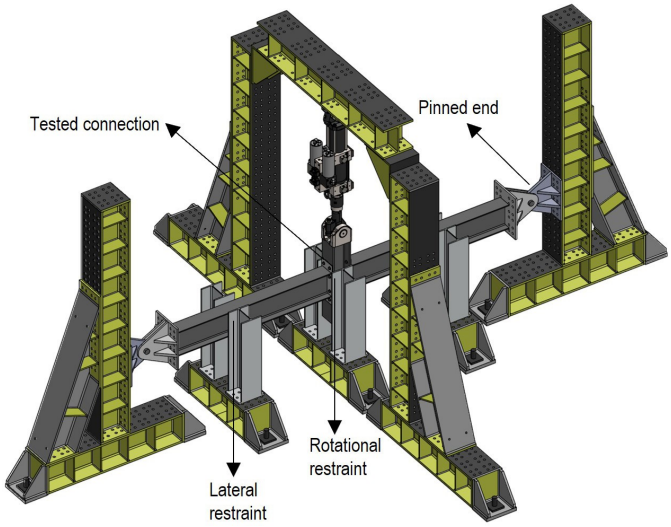

Fig. 5 The test arrangement for the quasi-static two-sided beam-to-column connection tests

3.2 Pre-test numerical modelling results

A numerical modelling study has been carried out prior to conducting the tests to predict the response of the specimens and to verify the capacity of the reaction frame system, the results of which are presented herein. The models were conducted in the finite element analysis package Abaqus [10]. The models were first validated against the results of similar tests on carbon steel connections conducted by Tan et al. [11,12]. For each of the connection types considered in this study, as presented in Fig. 6, both stainless steel and carbon steel models were considered to measure the relative performance of the two materials used in the connection parts. For the stainless steel connections, the plates and angles were austenitic EN 1.4307 and the bolts were fully threaded M16 grade A4-70, while for the carbon steel connections, the plates and angles were S275 and the bolts were fully threaded M16 grade 8.8. The models employed representative stress-strain responses for all the modelled components, which included post-ultimate and fracture stages for the bolts [13]. The same configurations as those shown in Fig. 6 were modelled for both stainless steel and carbon steel connections. The column is UC203×203×71 of length 1 m and the beam is UB 254×145×37 of length 2.3 m. The beam ends were assumed to be pinned. The obtained FE results in terms of the vertical and horizontal force versus vertical column displacement are shown in Fig. 7. The extended end plate, Fig. 7a, and the top and seat angle cleat, Fig. 7b, connections show the expected three stage response – namely (1) flexure dominated stage, at relatively small vertical displacements, where the behaviour and vertical load capacity is mainly by flexure action, (2) transition stage, where the response changes from flexure dominated to catenary dominated and (3) catenary dominated stage, at relatively large vertical displacements, where the vertical force is supported by the tensile catenary force developed in the beam. The

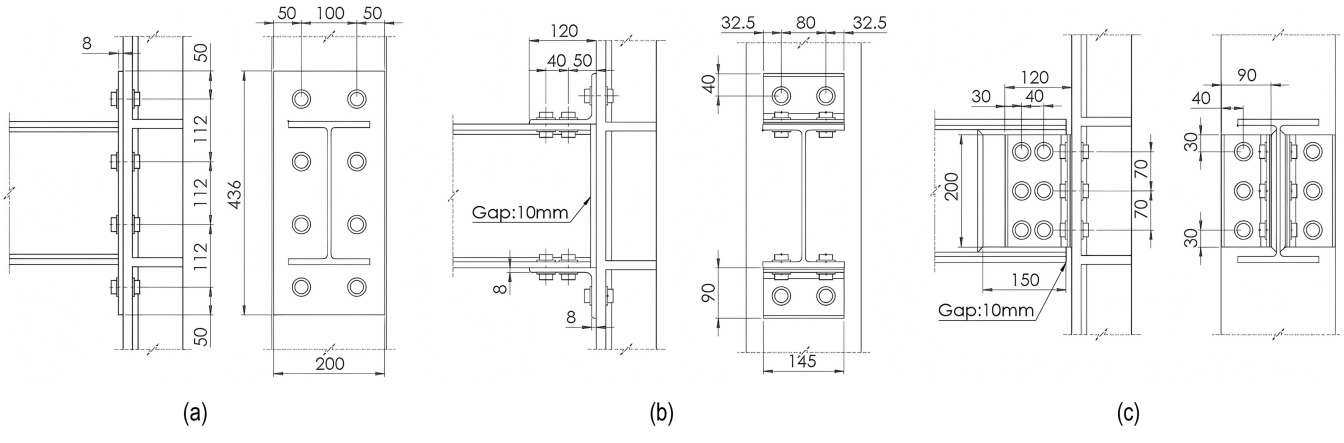

Fig. 6 Beam-to-column connection configurations; a) extended end plate; b) top and seat angle cleat; c) double angle web cleat

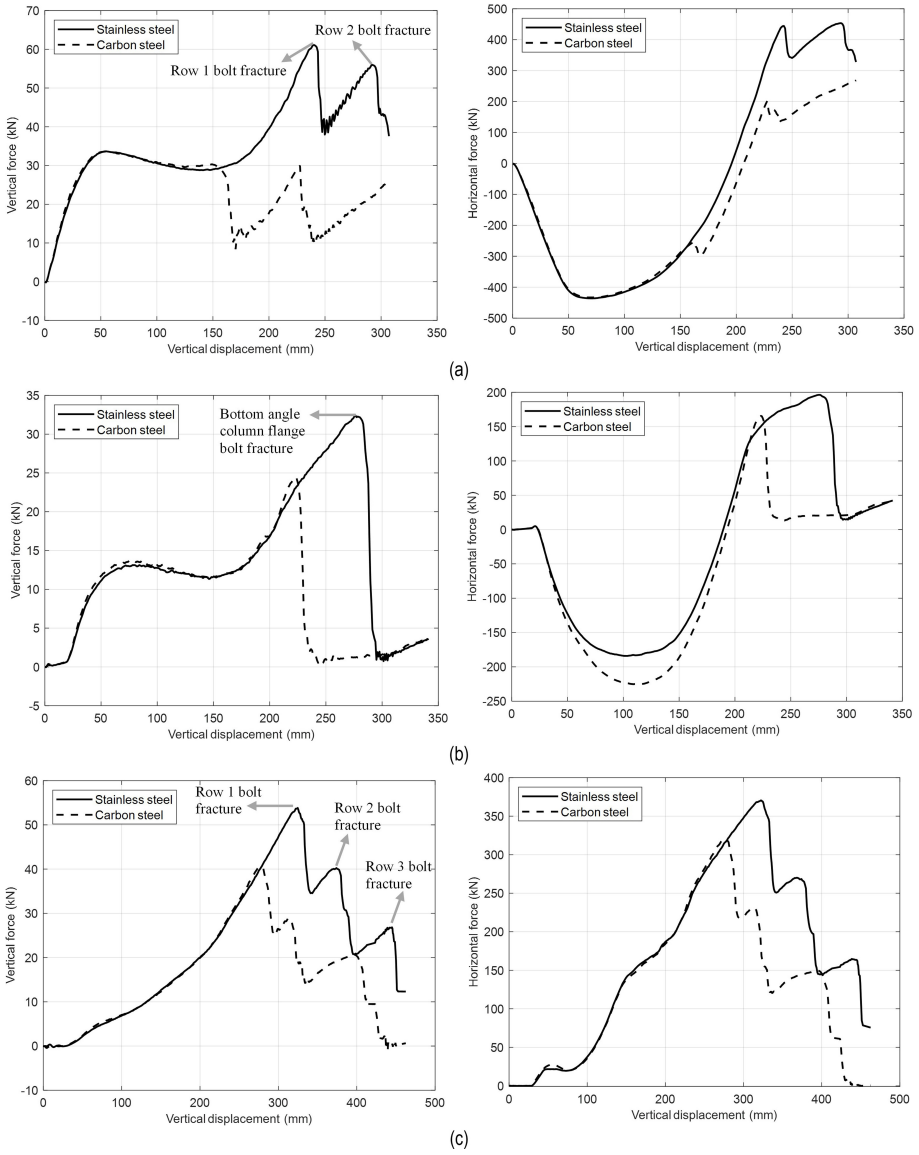

Fig. 7 Comparison of carbon steel and stainless steel quasi-static column removal responses; a) extended end plate connection, b) top and seat angle cleat connection, c) double web angle cleat connection

double web angle cleat connection resistance is purely by catenary action as shown in Fig. 7c. The failure modes of all the modelled connections was by tensile bolt fracture, which (*i*) for the end plate connection was the row one bolt tensile fracture followed by that of the row two bolt, (*ii*) for the top and seat angle cleat connection was the bottom angle column flange bolt fracture and (*iii*) for the double web angle cleat connection was rows 1, 2 and 3 bolt fracture consecutively as shown in as shown in Fig. 8a–c, respectively. In all cases, the stainless steel connections show enhanced load carrying capacity performance compared to the carbon steel connections of the same configuration. The vertical load resisted, at the point of first bolt fracture, are higher for the stainless steel connections by factors of about 2.0, 1.37 and 1.35 for the EEP, TAS and WA connections, respectively.

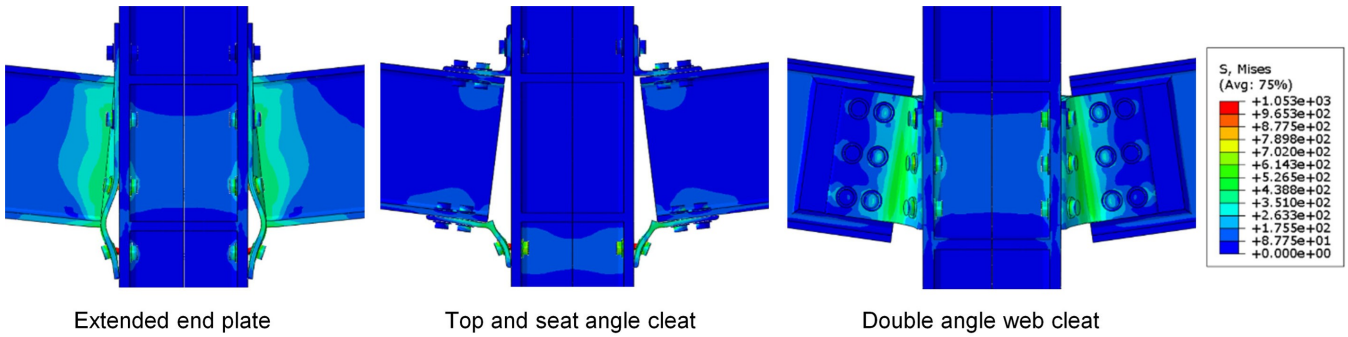

Fig. 8 FE predicted failure modes of the beam-to-column connections

4 Conclusions

This paper highlighted the advantages of the use of stainless steel in two cases involving extreme service environments, e. g. liquid hydrogen storage tanks, and loading conditions, e. g. steel-framed buildings subjected to accidental loadings. The material challenges associated to the transportation and storage of liquid hydrogen fuel at large-scale were presented and the use of stainless steel for design of storage vessels was discussed. The results of a pilot experimental programme investigating the tensile stress-strain behaviour of 304 L stainless steel under cryogenic 20 K temperature were presented and areas for further testing were identified. Under extreme loading conditions, stainless steel bolted connections were shown to possess higher load-carrying capacity and ductility resulting in enhanced structural robustness in case of a accidental loading conditions.

Acknowledgements

The research projects presented in this paper have received funding from *UK Research and Innovations* EPSRC (EP/W020351/1), the *Royal Academy of Engineering* under The Leverhulme Trust Research Fellowship Programme (LTRF2122-18-104), *Institution of Civil Engineers* Research and Development Enabling Fund and *The Southampton Marine and Maritime Institute*, which is gratefully acknowledged.

References

[1] HM Government (2021) UK Hydrogen strategy.
[2] Wang, Z.; Wang, Y.; Afshan, S.; Hjalmarsson, J. (2021) *A review of metallic tanks for H2 storage with a view to application in future green shipping.* International Journal of Hydrogen Energy 46, no. 9, pp. 6151–6179.
[3] Adolf, J.; Balzer, C. H.; Louis, J.; Schabla, U.; Fischedick, M.; Arnold, K.; Pastowski, A.; Schüwer, D. (2017) *Energy of the future?: Sustainable mobility through fuel cells and H2*; Shell hydrogen study.
[4] CEN. ISO 6892-4:2015. (2015) *Metallic materials – Tensile testing: Method of test in liquid helium*.
[5] Gardner, L. (2019) *Stability and design of stainless steel structures – Review and outlook.* Thin-Walled Structures 141. pp. 208–216.
[6] Spencer, K.; Embury, J.; Conlon, K.; Véron, M.; Bréchet, Y. (2004) *Strengthening via the formation of strain-induced martensite in stainless steels.* Materials Science and Engineering A 387, pp. 873–881.
[7] Zheng, C.; Yu, W. (2018) *Effect of low-temperature on mechanical behavior for an AISI 304 austenitic stainless steel.* Materials Science and Engineering A 710, pp. 359–365.
[8] Ding, H.; Wu, Y.; Lu, Q.; Wang, Y.; Zheng, J.; Xu, P. (2019) *A modified stress-strain relation for austenitic stainless steels at cryogenic temperatures.* Cryogenics 101, pp. 89–100.
[9] Ding, H.; Wu, Y.; Lu, Q.; Xu, P.; Zheng, J.; Wei, L. (2018) *Tensile properties and impact toughness of S30408 stainless steel and its welded joints at cryogenic temperatures.* Cryogenics 92, pp. 50–59.
[10] Abaqus (2014) *ABAQUS user's manual.* Version 6.14. Hibbitt, Karlsson & Sorensen, Inc. Pawtucket, RI.
[11] Yang, B.; Tan, K. H. (2013) *Experimental tests of different types of bolted steel beam-column joints under a central-column-removal scenario.* Engineering Structures 54, pp. 112–130.
[12] Yang, B.; Tan, K. H. (2012) *Numerical analyses of steel beam-column joints subjected to catenary action.* Journal of Constructional Steel Research 70, pp. 1–11.
[13] Song, Y.; Wang, J.; Uy, B.; Li, D. (2020) *Experimental behaviour and fracture prediction of austenitic stainless steel bolts under combined tension and shear.* Journal of Constructional Steel Research 166, pp. 105916.

Authors
Dr. Sheida Afshan (corresponding author)
s.afshan@soton.ac.uk
University of Southampton
Faculty of Engineering and Physical Sciences
Department of Civil, Environmental and Maritime Engineering
Southampton, UK

Weiran Li
wl2u20@soton.ac.uk
University of Southampton
Faculty of Engineering and Physical Sciences
Department of Civil, Environmental and Maritime Engineering
Southampton, UK

Dr. Zhenzhou Wang
zhenzhou.wang@soton.ac.uk
University of Southampton
Faculty of Engineering and Physical Sciences
Department of Mechanical Engineering
Southampton, UK

Dr. Wendell Bailey
w.o.s.bailey@soton.ac.uk
University of Southampton
Faculty of Engineering and Physical Sciences
Department of Mechanical Engineering
Southampton, UK

Dr. Yikun Wang
Yikun.Wang@lr.org
Lloyd's Register
Southampton, UK

How to Cite this Paper
Afshan, S.; Li, W.; Wang, Z.; Bailey, W.; Wang, Y. (2023) *High-performance metallic materials for applications in infrastructure and energy sectors*. Steel Construction 16, No. 3, pp. 144–150.
https://doi.org/10.1002/stco.202300025